Fabrication and Characterization of Proton Conductive Membranes Based on Poly(methyl methacrylate-co-maleic anhydride)

Nasiri, Mohammad; Atabaki, Fariborz*[+]

Department of Chemistry, Malek-Ashtar University of Technology, Shahin-Shahr, P.O. Box 83145-115 Isfahan, I.R. IRAN

Ghaemi, Negin

Department of Chemical Engineering, Kermanshah University of Technology, 67178 Kermanshah, I.R. IRAN

Seyedzadeh, Zahra

Department of Chemistry, Malek-Ashtar University of Technology, Shahin-Shahr, P.O. Box 83145-115 Isfahan, I.R. IRAN

ABSTRACT: *In this study, proton conductive composite membranes were produced by using a poly(methylmethacrylate-co-maleic anhydride) (P(MMA-co-MAH)) copolymer and phosphotungstic Acid (PWA) as an additive of the proton conductive agent. P(MMA/MAH) 70/30, 50/50, and 30/70 were synthesized using a free radical polymerization reaction. PWA with a concentration of 2% was added to improve the performance of proton exchange membranes. Composite membranes of P(MMA30-co-MAH70)/PWA had the highest performance, and this improvement was attributed to the presence of MAH and PWA. By increasing the ratio of MMA:MAH from 30/70 to 70/30, thermal stability, ion exchange capacity and proton conductivity of membranes enhanced up to 310°C, 0.85 meq/g, and 5.77 mS/cm, respectively. Moreover, the addition of PWA into the membrane matrix improved the membrane characteristics so that thermal stability, ion exchange capacity, and proton conductivity increased to 317°C, 0.98 meq/g, and 14.42 mS/cm. The synthesized copolymer offered the required properties to be used for the fabrication of a proton conductive membrane.*

KEYWORDS: *Proton conductive membranes; Copolymers; Fuel cells; Composites; Phosphotungstic acid.*

INTRODUCTION

Proton Exchange Membranes (PEMs) in hydrogen fuel cells attract more attention due to their high conversion efficiency [1] Polymeric Electrolyte Membranes (PEMs) are one of the key components for fuel cells [2-5]. In recent studies, fuel cell membranes should have the necessary mechanical and thermal strength in addition to the appropriate conduction of proton [5]. Nafion has always been considered as the best proton exchange

***** *To whom correspondence should be addressed.*
+ E-mail: atabaki@mut-es.ac.ir ; f.atabaki@gmail.com
1021-9986/2020/1/43-57 15/$/6.05

membrane, because of its characteristics, which include high proton conduction (in high relative humidity), high mechanical properties and commercial availability. In addition to the mentioned advantages for Nafion, some disadvantages such as high cost, low conductivity in low humidity or high temperatures have drawn the attention of scientists to other polymers [1, 3].

The polyoxometalate salts (POMs) are well-known metal–oxygen cluster compounds and received much attention in recent years owing to their high acid strength and thermal stability. POMs as a new kind of electrolytes with Keggin anion structure are well known superionic conductors in their fully hydrated states. Among POMs, phosphotungstic acid ($H_3PW_{12}O_{40}$, PWA) has the strongest acidity and proton conductivity [6-9].

Recently, the combination of the polymers for production of the membranes has been considered because of the improvement of chemical-physical thermoplastic properties or performance. The usage of composite membranes is a cost-effective way to improve the performance of the proton conductive membranes [10-14]. PMMA with the following properties, high mechanical strength and thermal and chemical stability [14], besides maleic anhydride (MAH) with the ability to form appropriate film and the unique feature of solubility in water, can supplement each other in providing the necessary properties for proton exchange of the membrane. Furthermore, polymers are available and inexpensive [15]. The collection of these features has led to the study of the various combinations of these two polymers [10-15].

Generally, the preparation of PMMA involves the formation of saturated end groups and head-to-head links (H-H) due to asymmetry and coupling reaction. These abnormal structures led to thermoplastics possibility (poor heat-up) for PMMA which requires the necessity of reformations. The addition of different types of modifiers to a polymer matrix is a common way to improve and modify its properties [10]. It has been known that various copolymers of MAH with other various compounds having high ionic exchange properties are used for provision of the selected membranes with water uptake capacity [1]. MAH is a unique monomer because they do not undergo homopolymerization easily, while they can form copolymers without any challenge. MAH ($C_4H_2O_3$) is a unique electron receptor monomer that is highly reactive with anhydride groups. As the numbers of polar, rigid or cyclic groups in the backbone of polymers increases, the chain-elasticity of the polymer decreases. On the other hand, interactions of the electron-accepting maleic anhydride groups with the charge-carriers are expected [11, 16]. They are hydrolyzed in the water and produce carboxylic poly-electrolytes whose behavior in aqueous solutions is mainly influenced by electrostatic reactions between poly-anions and solutions. This behavior is also affected by the structural characteristics of acid maleic copolymers such as the presence of two carboxylic acid adjacent groups in a maleic unit, the hydrophilic/hydrophobic property of the combinatorics, and the polymer configuration [17].

Copolymers and tripolymer of MAH due to the presence of active anhydride groups in the structure of this compound can be modified to be used in the considered cases. MAH is a reactive monomer, so its copolymers or tripolymers are known as reactive polymers [18, 19]. The anhydride units during the polymerization facilitate the reaction and form the active sites during the bonding and reformation. Many copolymers are used for various applications of synthesis when the properties of maleic anhydride are used [15]. MMA forms weak films meaning that it has low mechanical strength which can be improved in the presence of polymers with hardened groups by the formation of copolymers. MAH as a combiner with five-ring can provide the necessary hardness and create copolymer with excellent thermal characteristics [15, 17]. Reviewing the literature revealed that although the (P(MMA-co-MAH)) copolymer has been studied in the production of some membranes, there are no study on employing of these copolymers for fabrication of composite membranes with proton exchange application. The present study for the first time studied the fabrication of proton conductive composite membranes of P(MMA-co-MAH)/PWA. Hence, in the first stage, the synthesis of P(MMA-co-MAH) is focused by increasing the ratio of MMA: MAH from 30/70 to 70/30, respectively. In the next stage, the proton exchange membranes were fabricated. In order to improve the proton conductivity of membranes, PWA2% was added as an influential additive with the proton conductive agent into the composite membranes matrix. The structure and properties of synthesized polymers and membranes were studied using

FTIR, SEM, TGA, DTG, DSC, IEC, water uptake and AC impedance spectroscopy tests and with particular emphasis on the PEM related properties such as proton conductivity of membranes. It is expected, due to particular properties of PMAH and PWA with appropriate functional groups, the composite membranes present the desirable properties and efficiency in proton conductivity.

EXPERIMENTAL SECTION

Materials

Methyl methacrylate (MMA, Mw=100.12 g/mol, ρ=0.943 g/cm^3), ethyl acetate, benzoyl peroxide (BPO, Mw=242.23 g/mol), maleic anhydride (MAH, Mw=98.06 g/mol) and methanol were purchased from Merck, Germany. Phosphotungstic acid (PWA, MW=2800 g/mol), acetate and sodium hydroxide were supplied by Fluka, Switzerland. All the reagents and solvents were of analytical grade and used without further purification. Non-woven sheets were received from Coin Nanotech, Aldrich, China.

Synthesis of poly(methyl methacrylate-co-maleic anhydride) (P(MMA-co-MAH)s)

P(MMA-co-MAH)s in three weight ratios of 30/70, 50/50, and 30/70 from the monomers of MAH and MMA were synthesized via free radical copolymerization. It should be mentioned that another ratio 10/90 of MAH/MMA was also examined, but the oligomerization of the polymer occurred by reducing the amount of MAH and increasing the amount of MMA from 30/70 to 10/90 in the copolymer structure. Table 1 shows the combination of the composites. Copolymerization was started by adding BPO (1 wt.%) as the primer in the solvent of ethyl acetate at 80 to 90°C for 12 h under stirring conditions. The created pink solution was sedimented in methanol. A little amount of the obtained product with a dropper was poured out in a separate test tube containing methanol, acetone and toluene for solubility test. The obtained copolymers were dissolved in acetone and not methanol and toluene. On the other hand, a little amount of synthesized PMMA was poured out in the same solvents and it was observed that PMMA was soluble in acetone and toluene but insoluble in methanol. As a result, methanol was selected as the appropriate anti-solvent. The molecular structure of the copolymer P(MMA-co-MAH) is as shown in Fig. 1.

The obtained sediment was a mixture of copolymer P(MMA-co-MAH), unreacted MAH, homopolymer MAH, MMA, etc. Toluene was used to remove PMMA homopolymers which were still present in the obtained sediment. The obtained solution after 12 h of reaction was added to the container containing methanol at room temperature and was slightly stirred for precipitation. Decanter methanol and the obtained sediment were stirred for 15 min in order to separate the residual PMMA homopolymers and other impurities in the toluene to obtain copolymer with higher purity. The obtained pinkish-white sediment was filtered (smoothen) and dried in an oven at 40 to 50°C and washed with toluene. This process was repeated several times to obtain pure copolymer [5].

For all copolymerization reactions, 15 ml of ethyl acetate and 0.06 g of PBO were used. The reaction time was 12 h.

Determination of MAH content in P(MMA-co-MAH)s

Considering the effective role of MAH in improving the properties of synthesized copolymers, the amount of MAH content in copolymers was calculated using titration method. After performing titration for each sample based on the amount of consumption profit and using formulae 1 and 2, the amount of MAH that entered into the polymer chain can be calculated. The amount of the calculated MAH for the provided polymers is listed in Table 2. Approximately, 0.3 g of each copolymer with N, N-dimethylformamide (DMF, 12 mL) was completely dissolved at room temperature. The solution was then added to 0.3 ml aniline and was completely mixed for 1.5 h in order to perform the reaction of the aniline with the MAH carbonyl group. The solution was titrated with a standard solution of 0.05 mol/l NaOH in ethanol using the thymol blue indicator [20]. Color changes of the solution from yellow to green show the end point of titration. The following formula shows the amount of MAH that can be calculated in terms of the consumed volume of NaOH:

$$W\%_{MAH} = \frac{V_{NaOH}(mL) \times M_{NaOH}\left(\frac{mol}{L}\right)}{2 \times \frac{98\left(\frac{g}{mol}\right)}{W_g}} \times 100 \qquad (1)$$

Table 1: The materials amounts used for synthesis of P(MMA-co-MAH)s.

Copolymer	MMA (ml)	MAH (g)	Ultimate Sediment Weight (g)
P(MMA70-co-MAH30)	4.2	1.76	3.1
P(MMA50-co-MAH50)	3.0	2.94	5.35
P(MMA30-co-MAH70)	1.8	4.116	5.71

Table 2: The amount of the maleic anhydride content in the prepared copolymers.

	MAH%			
Copolymer	Theory (Wt%)	Experimental (Wt%)	Reagent amount (in the feed) (mol%)	Yield (%)
P(MMA70-MAH30)	0.09	0.09	30	52
P(MMA50-MAH50)	0.15	0.12	40	78.5
P(MMA30-MAH70)	0.21	0.20	66.6	89.2

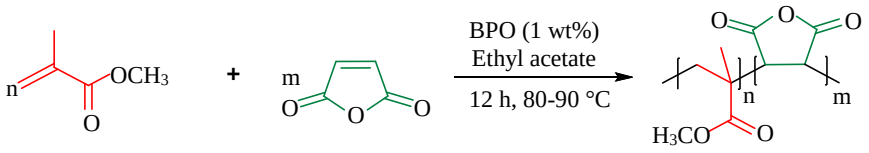

M= 30, 50, 70 mol% of n

Fig. 1: Synthesis procedure of P(MMA-co-MAH) copolymers.

where Wg is the using amount of polymers in titration.

The molar percentage of reacted MAH in copolymers can be obtained as:

$$(\text{Mole\%})\text{MAH} = \frac{\text{Wt}_{\text{MAH\%}}(\text{experimental}) - \text{Wm}_{\text{MAH\%}}(\text{Consumed in the feed})}{\text{Wt}_{\text{MAH\%}}(\text{theory})} \times 100 \quad (2)$$

Each aniline molecule invades to a carbonyl group from the MAH and opens the ring making the other side of the ring becomes acidic. The amount of MAH that entered into the copolymer was calculated by obtaining the amount of benefit that was used to neutralize the acidic portion of each MAH molecule. It can be concluded from the conducted calculations that the MAH monomer acceptably entered the polymeric chain and has a good compatibility with MMA.

Preparation of Membranes

All of the composite membranes were prepared using the solution-casting method [1]. In the first method, the solutions of copolymer P(MMA-co-MAH)s with three weight ratios of MMA/MAH were prepared in ethyl acetate solution at 400 rpm speed at room temperature, as shown in Table 3. In the second stage, in order to increase the performance of the proton exchange membranes, 2 wt.% PWA was added to the copolymer solutions with the same weight ratios and after complete dissolving of PWA, the solution was sonicated at room temperature for 15 min. Finally, the solutions were casted on the non-woven paper with 150 µm thickness at room temperature and for complete and gradual departure of the solvent it was placed under bung for 24 h.

Fourier Transform InfraRed (FT-IR) spectroscopy

Fourier Transform InfraRed (FT-IR) spectra of the samples were measured in absorbance mode by the spectrophotometer (Shimadzu FT-IR, Japan) with a temperature control cell. The spectra were all measured in the range of 500-4000 cm^{-1} at a resolution of 4 cm^{-1}.

Ion Exchange Capacity (IEC)

The ion exchange capacity (IEC) represents the number of ions' equivalent per gram of dried polymer. To determine the IEC, titration method was used.

Table 3: The composition of P(MMA-co-MAH) composite membranes.

Membrane Name	MMA/MAH	PWA (wt.%)
P(MMA70-co- MAH30)	70/30	0
P(MMA50-co- MAH50)	50/50	
P(MMA30-co- MAH70)	30/70	
P(MMA70-co- MAH30)/PWA	70/30	2
P(MMA50-co- MAH50) /PWA	50/50	
P(MMA30-co- MAH70) /PWA	30/70	

A small piece of each membrane was placed in a 0.1 mol of NaCl solution for 24 h to replace all H^+ with Na^+. This issue led to the changing of membrane from acidic condition to salty condition [22]. Then, the exchanged proton of solution was titrated with NaOH normal 0.001 solutions. The ion exchange capacity was calculated from Eq. (3):

$$EC = \frac{C_{NaOH} \times V_{NaOH}}{M_{sample}} \quad (3)$$

In this equation, C_{NaOH} is the concentration of *NaOH* (mol/L), V_{NaOH} is the volume of NaOH consumed in the neutralization (mL), and M is the weight of dry membrane (g). Titration was repeated twice for each sample.

Water uptake (Wu)

The amount of water uptake has a direct relationship with the performance of the proton exchange membrane. Membrane water uptake was identified by measuring the changed weight before and after hydration [23]. All the specimens were completely dried at 40°C for 48 h in the dryer. The membranes were then placed in distilled water at ambient temperature for 24 h and then were dried on membrane surface with a filter paper, and the precise weight of wet membrane was determined using an accurate scale. The membranes were then placed at 40°C for 16 h and the weight of the membrane was reweighed. Water uptake percentage was calculated using Eq. (4):

$$\text{Water uptake} = \frac{Ww - Wd}{Wd} \times 100\% \quad (4)$$

In this equation *Ww* is the wet membrane weight and *W*d is the dry membrane weight.

Proton conductivity

This test is one of the most important tests to find the relationship between the structure and the function of the material because determining the final composition plays an important role in the proton conduction of the membrane. Proton conductivity is measured by measuring the proton conductive membrane resistance based on Alternating Current (AC) or direct current [24]. In this study, membranes with the dimension 1 cm × 1 cm were cut and conductivity was determined by measuring the AC impedance using (Hioki 3560 AC Miliohm hitester- HFR meter, AHNS Co.). Samples were placed inside the cell; this cell is connected to the device by two electrodes, and the oscillating potential of 10 mV was applied in the frequency range of 100 kHz to 10 Hz. The considered mass resistance in the membrane thickness was obtained from the highest frequency of intersection of the virtual component of the impedance with the real axis [1, 5, 25].

Then, the proton conduction was calculated using Eq. (5):

$$\sigma = \frac{L}{RS} \quad (5)$$

In this equation, σ is the proton conduction (s/cm), L is the thickness of the membrane (cm), R is the resistance (Ω), and S is the area of the membrane which is testing (cm^2).

Thermal analysis

Thermal properties of the prepared copolymers and membranes were examined using the device of ThermoGravimetric Analysis (TGA), Differential ThermoGravimetric analysis (DTG) made in the Perkin Elmer Company, Diamond Model, and Differential Scanning Calorimetry (DSC) under argon conditions

with a heating rate of 10°C/min from ambient temperature up to 700°C using the Perkin Elmer system of the Pyris 6 DSC model.

RESULTS AND DISCUSSION

FT-IR analysis

FT-IR spectrum (Fig. 2) was used to determine the formation of P(MMA-co-MAH) in different ratios of MMA/MAH and PWA monomers. P(MMA-co-MAH)s copolymers have peaks at the wavelengths of 1850 and 1786 cm^{-1} representing the symmetric and asymmetric tensile vibration of the anhydride unit $C=O$, respectively [1, 2, 16, 20]. One of the characteristics of the anhydride five-ring is being $(O=C-O-C=O)$ which is about 950 cm^{-1}. These results show that maleic anhydride exists in the combination of copolymers successfully [20].

Strong tensile vibration of $O-C=O$ of carbonyl ester belonging to the MMA group was observed at 1728 cm^{-1} [2, 10, 20]. The three carbonyl characteristic peaks of the MMA and MAH groups appear near each other [16]. The peak area of 2953 cm^{-1} shows the $C-H$ tensile vibrations of the MMA and MAH. In addition, the peaks of 1453 and 1385 cm^{-1} show asymmetric and symmetric bending vibrations of the $-CH_3$ and $-OCH_3$ groups of the MMA group [2, 10, 26]. Therefore, from spectra comparison, it can be ensured that copolymerization of MMA and MAH occurred in different proportions.

Thermal analysis

Figs. 3 and 4 show the TGA and DTG curves of P(MMA-co-MAH)s with different ratios and their data are shown in Table 4.

The thermal analysis for this copolymer shows the improvement of its thermal stability relative to pure PMMA. Thermal decomposition of copolymers is generally performed in two steps. At the first step, at the temperatures of about 100 to 120°C, the moisture and impurities were removed from copolymers. After removing moisture, at the second step, dry copolymers were decomposed into smaller components such as methane, methanol, water, and CO_2 gas. The degradation temperature of dried copolymers (T_2) with 70, 50 and 30% MAH ratios is 272, 267 and 254°C, respectively which shows the thermal stability of copolymer

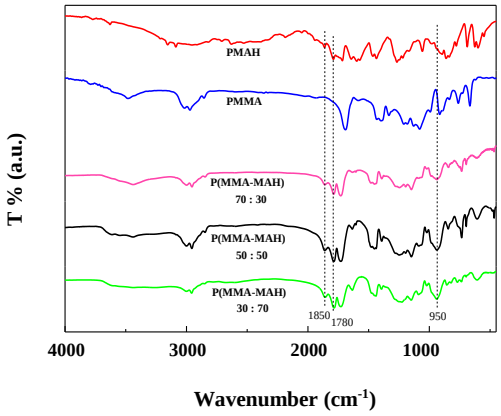

Fig. 2: The FT-IR spectra for PMMA, PMAH and the P(MMA-co-MAH)s.

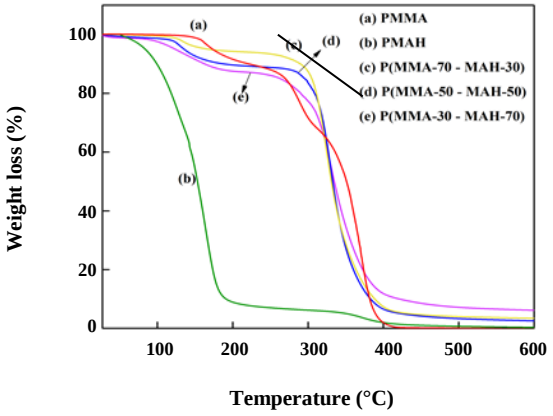

Fig. 3: TGA curves of PMMA, PMAH and P(MMA-co-MAH)s.

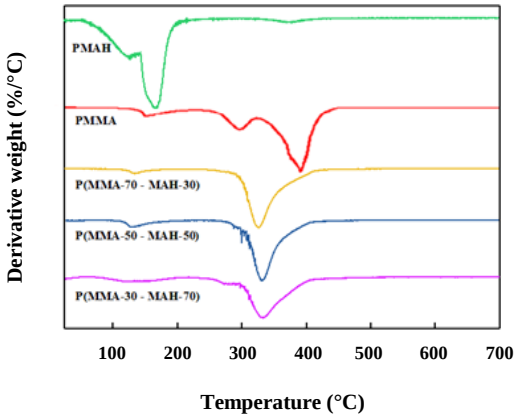

Fig. 4: DTG curves of PMMA, PMAH and P(MMA-co-MAH)s.

Table 4: Thermal Properties of P(MMA-co-MAH)s.

MMA%	MAH%	T_{10} (°C)	T_{50} (°C)	Char yield (%)	Tg (°C)	Yield (%)
100	--	221	351	0.80	104	85.0
70	30	289	329	1.61	139	52.0
50	50	189	331	1.00	142	78.5
30	70	161	332	5.00	146	89.2
--	100	99	152	1.10	115	40.0

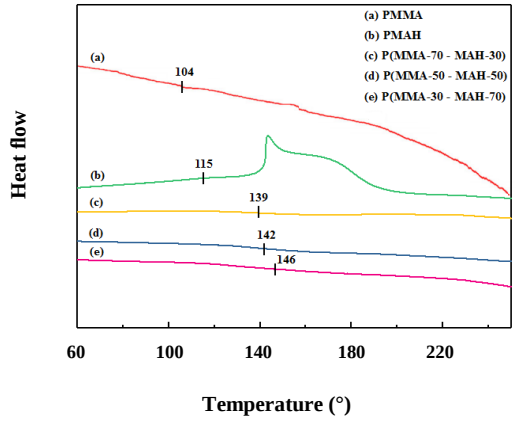

Fig. 4: DSC curves of PMMA, PMAH and P(MMA-co-MAH).

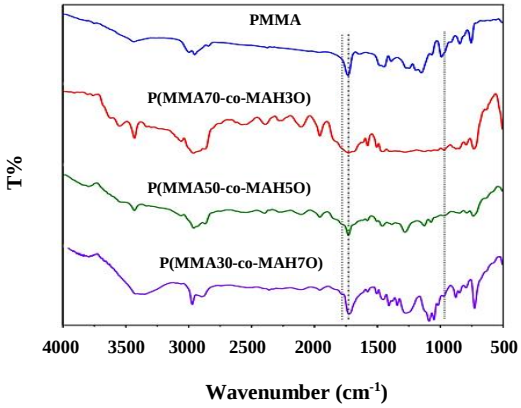

Fig. 6: FT-IR spectra of PMMA and P(MMA-co-MAH) membranes.

(MMA30-co-MAH70) in comparison with other copolymers and PMMA with the degradation temperature of around 250°C [26]. Thermal degradation temperature of 50% copolymers (T_{50}) containing 70, 50 and 30% MAH is 332, 331, and 329°C, respectively. At the end of the thermal decomposition, coagulation efficiency for copolymer containing 70% MAH at the temperature of 600°C was about 5% proving the higher thermal stability of this copolymer compared with PMMA and other copolymers. The presence of MAH monomer improves the coagulation efficiency; this has also been proven in other reports [27]. Therefore, higher amount of MAH was effective in improving of the thermal stability.

DSC charts of P(MMA-co-MAH) copolymers are also shown in Fig. 5. All copolymers have a Tg indicating that these copolymers have dominantly uniform and homogeneous monomer distribution. Compared to PMMA and PMAH, Tg values for copolymers containing 70% MAH are higher (about 146°C); this is a significant increase in the PMMA glass transition temperature. It can be inferred that increasing the amount of MAH increased Tg. Therefore, the connection of MAH monomers to the main chain was performed randomly and effectively by delaying the movement of polymer chains.

Evaluation of P(MMA-co-MAH)/PWA composite membrane properties

The main objective of this project was to prepare proton conductive membranes. The membranes were fabricated to produce a proton conductive composite membrane from P(MMA-co-MAH)s electrolyte and PWA as an inorganic acid compound and reinforcement agent of the proton conduction system.

FT-IR spectra of PMMA and P(MMA-co-MAH) membranes are presented in Fig. 6.

P(MMA-co-MAH)s copolymers contain anhydride units at the wavelengths of 1786 and 1850 cm^{-1} showing the $C=O$ tensile vibrations of symmetric and asymmetric, respectively [1, 2, 16, 20]. In addition, the characteristic peak of the anhydride with 5-square ($O=C-O-C=O$) which is about 950 cm^{-1} shows that the MAH has been successfully entered to the copolymer

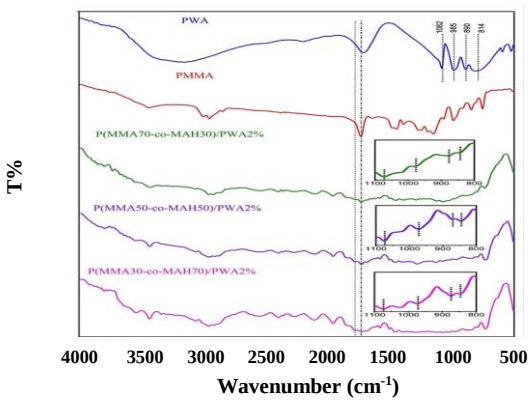

Fig. 7: FT-IR spectra of PWA, PMMA and P(MMA-co-MAH)/PWA composite membranes.

structure. The tensile vibrations of the carbonyl ester group of the MMA ($O-C=O$) groups are located in the 1720 cm^{-1} region [2, 10, 20]. Three $C=O$ characteristic peaks of MAH and MMA appear near each other [16, 28]. The peak of 2952 cm^{-1} shows the C-H tensile vibrations of MMA and MAH. Moreover, the appeared peaks at 1453 and 1365 cm^{-1} show the asymmetric and symmetric bending vibrations of $-CH_3$ and $-OCH_3$ of MMA units [10, 26]. Therefore, the MAH-co-MMA copolymer forms the membrane matrix. In comparison (MMA-co-MAH)s copolymer membranes spectrum some minor changes are observed in the shape and position of copolymer membranes peaks, due to the presence of polymer groups in the structure of the membrane.

The characteristic peaks of the copolymer in relation to the MAH and MMA groups are also visible in (MMA-co-MAH)s membrane and P(MMA-co-MAH)/PWA composite membrane spectra (see Fig. 7).

Peaks in the range of 1500 -1600 cm^{-1} (symmetric and non-symmetric concentration vibrations) $-COO^-$ are in the $-COOH$ group. Flat peaks ranging from 1750 to 1800 $C=O$ cm^{-1} are in the $-COOH$ group that overlaps with the ester peak [1]. In the FT-IR spectrum, the characteristic peaks of pure PWA groups appeared at 814 to 1080 cm^{-1}. In addition, all PWA peaks are as shown in Fig. 7 in the P(MMA-co-MAH)/PWA composite membrane spectrum. The PWA spectrum shows absorption bands at about 1080 cm^{-1} ($P-O$ in central tetrahedral), 985 cm^{-1} (terminal $W=O$), 890 cm^{-1} and 814 cm^{-1} ($W-O-W$) associated with the asymmetric vibrations in Keggin polyanions [8, 29].

To compare the (MMA-co-MAH)/PWA composite membrane spectrum, some changes are observed in the shape and position of PWA peaks due to the interaction of the Keggin structure from PWA molecules and agent groups in the polymer structure of the membrane. The interaction between the operation groups of copolymer, carbonyl groups (MAH and MMA), $-COO^-$ and PWA consists of oxygen atoms and water molecules, transfer proton simultaneously by the formation of hydrogen bond and diffusion of hydrolyzed water molecules in PWA structure [30].

Thermal analysis

From the results of previous studies, the presence of MAH monomer improved the thermal properties of copolymers and since PWA mineral particles are expected to improve some copolymer properties, the prepared membranes were identified and they were also studied in term of thermal stability using TGA, DTG and DSC methods. Thermal studies of the prepared membranes are shown in Table 5. In Fig. 8, the thermal stability of P(MMA-co-MAH)s membranes and the composite membranes with PWA are shown in various ratios of copolymers (MMA/MAH) 30/70, 50/50, and 70/30. All membranes showed a two-step degradation pattern.

The first step of the P(MMA-co-MAH)s membrane weight loss at temperature around 100°C is related to the removal of moisture and impurities from the membrane polymer structure. After removal of moisture, the second step of degradation has to do with the decomposition of the copolymers forming the membrane matrix into smaller components. The starting temperature of the second degradation step for membranes prepared of 30, 50 and 70% copolymers of MAH is about 299, 307, and 310°C, respectively. As shown, the thermal stability in the membranes improved by increasing the ratio of MAH to MMA. The TGA chart shows that the P(MMA-co-MAH)/PWA composite membranes have two different degradation steps. The first step is due to the removal of moisture from the structure of copolymers and the removal of water from the PWA structure [31]. The starting temperature of the second degradation step is in the range of 310 to 315°C; this parameter is higher compared to the membranes prepared with the same composition but without PWA which in turn makes

Table 5: Thermolysis information of P(MMA-co-MAH)/PWA composite membranes.

Tg (°C)	Char yield (%)	T_{50} (°C)	T_{10} (°C)	MAH%	MMA%	PWA %	T_{i2} (°C)
126	3	360	325	30	70	0	299
130	4	360	335	50	50	0	307
142	7	365	255	70	30	0	310
144	21	357	177	30	70	2	310
146	25	370	190	50	50	2	315
149	27	370	182	70	30	2	317

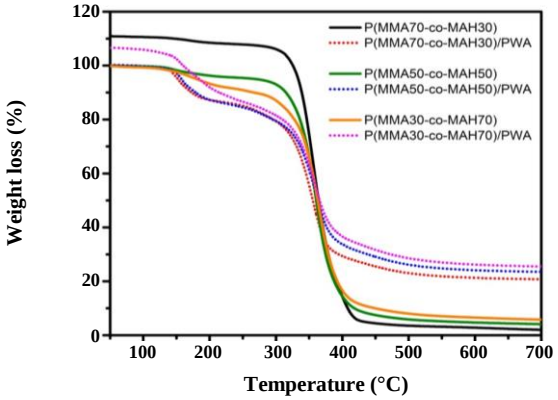

Fig. 8: TGA curves of P(MMA-co-MAH) and P(MMA-co-MAH)/PWA composite membranes.

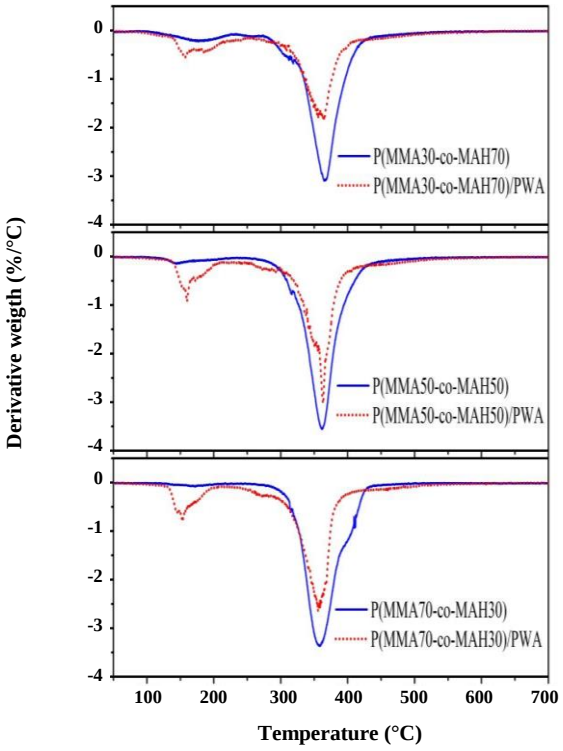

Fig. 9: DTG curves of P(MMA-co-MAH) and P(MMA-co-MAH)/PWA composite membranes.

the composite membranes stable. The second step of thermal decomposition is the destruction of the polymeric network, the structure of PWA, and the elimination of interactions between the PWA groups and the copolymer. Thermal stability of T_{50} improved slightly in composite membranes as compared to non-PWA membranes. These results show a particular interaction between PWA and copolymer functional groups helping to increment of thermal stability of composite membranes. [32].

Fig. 9 shows the DTG diagrams for different membranes. At the end of the thermal degradation, the coagulation efficiency for the composite membranes containing 30, 50, and 70% of MAH was 21, 25, and 27 %, respectively. These values were higher compared to the copolymer membranes prepared without PWA and with the same MAH ratios. It shows that the addition of PWA into the membrane matrix improved the thermal stability of the membranes up to the temperature around 700°C.

Composite of copolymers degraded at 700°C completely, but some parts of copolymers remained at the end of thermolysis. It exhibits that existence of more PWA units in the backbone was effective, and P(MMA-co-MAH)/PWA composite copolymer offered better thermal stability than poly(MMA-co-MAH). This means that the presence of PWA in the copolymer was influential on the copolymer thermal stability as a result of specific interactions between active groups of copolymer and functional groups of PWA [32, 33].

The highest thermal degradation rate (T_{max}) for the P(MMA-co-MAH)/PWA composite membrane with the highest percentage of MAH (70%) is about 365°C which shows the maximum thermal resistance compared to the membrane prepared without PWA with the same composition and other composite membranes.

The DSC chart for the prepared membranes are shown in Fig. 10. In all the (MMA-co-MAH)/PWA

Table 6: Water uptake of P(MMA-co-MAH)/PWA composite membranes.

Membrane Name	MMA/MAH	PWA (wt.%)	Water uptake (%)
P(MMA70-co- MAH30)	70/30	0	25±2
P(MMA50-co- MAH50)	50/50		47±1
P(MMA30-co- MAH70)	30/70		64±1
P(MMA70-co-MAH30)/PWA	70/30	2	33±1
P(MMA50-co-MAH50)/PWA	50/50		53±2
P(MMA30-co-MAH70)/PWA	30/70		76±2

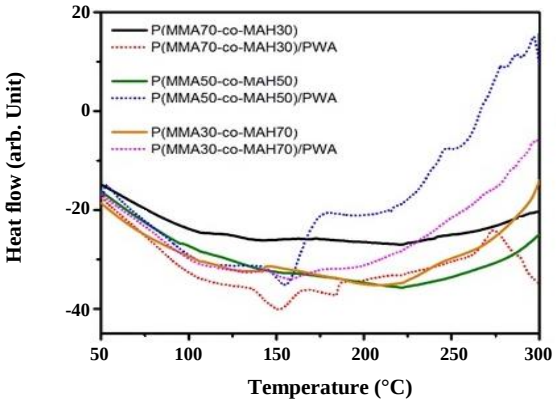

Fig. 10: DSC curves of P(MMA-co-MAH) and P(MMA-co-MAH)/PWA composite membranes.

membranes, increasing the amount of MAH in the copolymer structure and also adding 2% PWA led to increase in Tg. This increment can be attributed to the presence of repetitive units of MAH monomers in polymer matrix and interactions between the copolymer functional groups and PWA in the form of hydrogen bonds.

Water absorption and ion exchange capacity of P(MMA-co-MAH)/PWA composite membranes

Water uptake is one of the parameters that influence on the proton conduction in the ion exchange membrane. From the results in Table 6, in each combination, increasing the ratio of MAH to MMA and addition of PWA as the proton conduction agent increased the amount of water uptake. The reason is due to PWA acidic nature [32]. Although, COOH and OH groups created in the membrane structure would be beneficial in water uptake; the existence of PWA active functional groups in the membrane composition plays a very important role via forming the hydrogen bonds with the copolymer functional groups. These free volumes may trap more water molecules and increase the effective uptake of water. Such interaction was previously reported as well [19]. There is no doubt that there is a direct relation between water uptake and proton exchange capability of membranes, and hence, it is expected that an improvement in the proton conductivity of membranes is observed. [32, 34, 35].

The ion exchange capacity as an important parameter of conductivity and transfer capability of membrane shows the amount of charge density in the membrane. Table 7 shows the ion exchange capacity of the different combinations based on the ratio of MMA to MAH, and also the PWA in each combination.

As shown in Fig. 11, when MAH ratio in the copolymer combination increased, the ion exchange capacity enhanced as well. This result is due to the increment in the number of $-COO^-$ groups in each membrane. Acid groups are the most important factors in the proton transportation. The more the number of these groups, the more the amount of free H^+ that increases the ion exchange capacity. When PWA was added, ion exchange capacity increased. This matter is as a result of the formation of hydrogen bonds between the copolymer functional groups and PWA which increases the pathway for proton transfer. Since copolymers do not have acidic nature, by adding IEC and PWA, the acidity improves as a result of the enhancement in the H^+ ions [8]. Therefore, IEC value indicates the density of replaceable ions (H^+) which to some extent controls the proton transport especially the Grotthuss type [33, 40].

In this study, the ion exchange capacity was obtained in the range of 0.38 to 0.98 ($meqg^{-1}$) and the best value was related to P(MMA-co-MAH)/PWA membrane. These results proved the positive effect of MAH and PWA on improving the activated sites responsible

Table 7: Ion exchange capacity of the P(MMA-co-MAH) membranes.

Membrane Name	MMA/MAH	PWA (wt.%)	Ion exchange capacity (meq g^{-1})
P(MMA70-co- MAH30)	70/30	0	0.38±0.02
P(MMA50-co- MAH50)	50/50		0.58±0.01
P(MMA30-co- MAH70)	30/70		0.85±0.01
P(MMA70-co-MAH30)/PWA	70/30	2	0.47±0.02
P(MMA50-co- MAH50)/PWA	50/50		0.79±0.01
P(MMA30-co- MAH70)/PWA	30/70		0.98±0.02

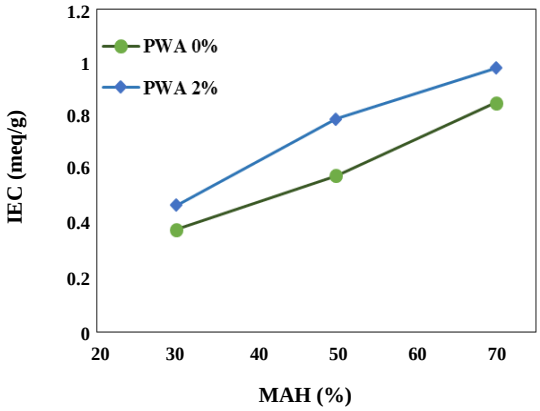

Fig. 11: Effect of MAH and PWA on the ion exchange capacity of membranes.

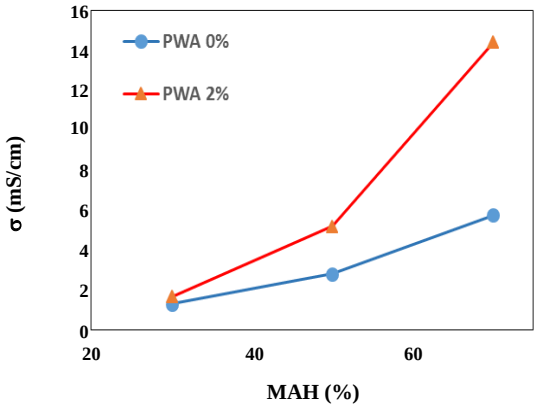

Fig. 12: Effect of MAH and PWA on the proton conductivity of membranes.

for the proton conduction and the creation of proton transfer pathways in the membrane.

Proton conduction of P(MMA-co-MAH) membranes

The result of proton transfer of the proton exchange membranes can be analyzed by using water uptake data and ion exchange capacity. To be a good conductor of the proton, a solid electrolyte should have active positions surrounded by water molecules that facilitate the transfer of protons. The proton conductivity of fuel cell membranes is closely related to the water content capacity [1]. Fig. 12 illustrates the changes in the conduction of proton membranes.

Hydrogen bonds between the groups of the proton receptor ($C=O$ anhydride or $-O-$ ether) and the proton giver ($-COO^-$) in the copolymer structure, and also the mutual bonds between the MAH groups and the PWA functional groups play an important role in the proton conduction rate which concurrently increases based on the vehicle-type and the Grotthuss-type mechanisms [33]. Under the Grotthuss mechanism, the mobility of protons is determined by the formation of hydrogen bond between a hydronium ion ($H_5O_2^+$, $H_7O_3^+$, $H_9O_4^+$, etc.) and another molecule or ion. On the other hand, proton might also transfer by diffusion of hydrolyzed water molecules in PWA structure. In this mechanism, proton diffuses through a vehicle such as H_2O (as H_3O^+) [30, 36-39]. Note that the mutual reactions of the copolymer connection with each other and the PWA functional group increase with change in copolymer ratio [1, 41]. [29]. As shown, in all three copolymer combinations, when the MAH ratio increased, the proton conduction improved because the amount of active $-COO^-$ groups increased. Hydrogen bonds of acid groups ($-COOH\ldots O=C$) of malic acid and MMA and the PWA functional groups make the proton exchange paths. These hydrophilic situations increase water uptake which in turn increases the amount of active proton in sites. The addition of PWA into the membrane matrix increases the inter-molecular hydrogen bonds.

Table 8: Proton conductivity of P(MMA-co-MAH) membranes.

Membrane Name	MMA/MAH	PWA (wt.%)	Proton conductivity ($mS.cm^{-1}$)
P(MMA70-co- MAH30)	70/30	0	1.32
P(MMA50-co- MAH50)	50/50		2.82
P(MMA30-co- MAH70)	30/70		5.77
P(MMA70-co-MAH30)/PWA	70/30	2	1.7
P(MMA50-co-MAH50)/PWA	50/50		5.22
P(MMA30-co-MAH70)/PWA	30/70		14.42

Providing more H^+ ions increases the movements of H_3O^+ free ion as the protons are needed to increase the efficiency of the proton exchange membrane and to improve the proton transfer. This free volume may absorb more water molecules and increase the water uptake in the membrane. Thus, the penetration and displacement of protons increase in the membrane structure via free water molecules and functional groups associated with PWA and copolymer (membrane matrix).

As shown in Table 8, the rise in the amount of MAH to 70% in the copolymer structure increases the proton conductivity to 5.77 $mScm^{-1}$. The addition of 2 wt.% PWA to this structure increases the proton conductivity to 14.42 $mS.cm^{-1}$.

CONCLUSIONS

In this study, P(MMA-co-MAH) copolymers were synthesized with different ratios of MMA and MAH monomers (70/30, 50/50, and 30/70) using the method of free radical copolymerization. The thermal analysis of the copolymers showed that MAH content played an important role in increasing the thermal resistance of copolymer P(MMA-co-MAH) copolymers.

The method of polymeric solution casting on the non-woven paper was used to prepare P(MMA-co-MAH)/PWA membranes with the same three ratios of the MAH/MMA and PWA combination. Improvement of membrane performance was investigated by adding PWA and increasing the amount of MAH in the membrane structure. By increasing the ratio of MAH to MMA in copolymer combination, the thermal stability, water uptake, ion exchange capacity and proton conduction increased significantly in the membranes. Also, the addition of PWA to the matrix of all the membranes was considerably effective on the improvement of all the parameters. All membranes showed a two-step degradation pattern. Increasing the amount of MAH in the presence of PWA improved the degradation resistance; this implies a particular interaction between the functional groups of PWA and copolymer in terms of hydrogen bonds. The connection of the MAH monomers to the main chain effectively delayed the movement of the polymer chains and thus, improved the thermal stability. On the other hand, improvement in the performance of the proton conductive membrane in the presence of the maximum content of MAH and PWA monomers was as a result of an increase in the amount of $-COO^-$ groups in the copolymer structure. In other words, increasing the amount of free H^+ increased the pathway for proton transfer due to the formation of hydrogen bonds between the copolymer and PWA functional groups. By increasing the MAH value to 70% in the copolymer structure, the proton conductivity increased to 5.77 $mScm^{-1}$. The addition of 2 wt.% PWA to this structure increased the proton conductivity to 14.42 $mScm^{-1}$ which was about two and half times of the initial value.

Received : May 29, 2018 ; Accepted :Nov. 5, 2018

REFERENCES

[1] Mandanipour V., Noroozifar M ., Modarresi-Alam A. R., Fabrication and Characterization of a Conductive Proton Exchange Membrane Based on Sulfonated Polystyrenedivinylbenzene Resin-Polyethylene (SPSDR-PE): Application in Direct Methanol Fuel Cells, *Iran. J. Chem. Chem. Eng.(IJCCE)* , **36**: 151-162 (2017).

[2] Yue W.-W., Xiang T., Zhao W.-F., Sun S.-D., Zhao C.-S., Preparation and Characterization of pH-Sensitive Polyethersulfone Membranes Blended with Poly (methyl methacrylate-co-maleic anhydride) Copolymer, *Sep. Sci. Technol.*, **48**: 1941-1953 (2013).

[3] Bhavani P., Sangeetha D., Blend Membranes for Direct Methanol and Proton Exchange Membrane Fuel Cells, *Chin. J. Polym. Sci.*, **30**: 548-560 (2012).

[4] Shi J., Composite Membranes for Proton Exchange Membrane Fuel Cells, *Wright State University*, 836 (2008).

[5] Askari M.M., Pourhossaini. M R, and Solimannia. S, Polyvinyl Alcohol-Sulfonated Polyethersulfone Blend for Application in Proton-Exchange Membrane, *Iran. J. Polym. Sci. Technol*, **29**(5): 403-412 (2016).

[6] Gomes F.N., Mendes F.M., Souza M.M., Synthesis of 5-Hydroxymethylfurfural from Fructose Catalyzed by Phosphotungstic Acid, *Catal. Today*, **279**: 296-304 (2017).

[7] Kim Y., Shanmugam S., Polyoxometalate–Reduced Graphene Oxide Hybrid Catalyst: Synthesis, Structure, and Electrochemical Properties, *ACS Appl. Mater. Interfaces*, **5**(22): 12197-12204 (2013).

[8] Zhou Y., Yang J., Su H., Zeng J., Jiang S.P., Goddard W.A., Insight Into Proton Transfer in Phosphotungstic Acid Functionalized Mesoporous Silica-Based Proton Exchange Membrane Fuel Cells, *J. Am. Chem. Soc.*, **136**(13): 4954-4964 (2014).

[9] Lu S., Wu C., Liang D., Tan Q., Xiang Y., Layer-by-Layer Self-Assembly of Nafion–[CS–PWA] Composite Membranes with Suppressed Vanadium Ion Crossover for Vanadium Redox Flow Battery Applications, *RSC Adv.*, **4**: 24831-24837 (2014).

[10] Xiao L., Li Z., Dong J., Liu L., Shang L., Zhang X., Zhang H., Ao Y., Dong A., Fabrication of Poly (methyl methacrylate-co-maleic anhydride) Copolymers and Their Kinetic Analysis of the Thermal Degradation, *Colloid. Polym. Sci.*, **293**(10): 2807-2813 (2015).

[11] Huang Y., Ma X., Liang G., Wang S., Gel Polymer Electrolyte Based on the Synthesized co-Polymer of Poly (methyl methacrylate-maleic anhydride), *Clays Clay Miner.*, **43**(3): 405-413 (2008).

[12] Jo C., Pugal D., Oh I.-K., Kim K.J., Asaka K., Recent Advances in Ionic Polymer–Metal Composite Actuators and Their Modeling and Applications, *Prog. Polym. Sci.*, **38**(7): 1037-1066 (2013).

[13] Hasani-Sadrabadi M.M., Dashtimoghadam E., Ghaffarian S.R., Sadrabadi M. H. H., Heidari M., Moaddel H., Novel High-Performance Nanocomposite Proton Exchange Membranes Based on Poly (ether sulfone), *Renewable Energy*, **35**(1): 226-231 (2010).

[14] Boztuğ A., Yılmaz E., Effects of Reactive Terpolymer Containing Maleic Anhydride on Thermomechanical Properties of Poly (vinyl chloride) Based Multicomponent Blends, *Mater. Res. Innovations*, **29**: 158-160 (2013).

[15] Boztuğ A., Basan S., Modification and Characterization of Maleic Anhydride-Styrene-Methyl Metacrylate Terpolymer Using Various Alcohols, *Designed Monomers and Polymers*, **9**: 617-626 (2012).

[16] Karakus G., Zengin H.B., Polat Z.A., Yenidunya A.F., Aydin S., Cytotoxicity of Three Maleic Anhydride Copolymers and Common Solvents Used for Polymer Solvation, *Polym. Bull.*, **70**: 1591-1612 (2013).

[17] Chitanu G., Rinaudo M., Desbrières J., Milas M., Carpov A., Behavior of Nonalternating Maleic Acid Copolymers in Aqueous Solution, *Langmuir*, **15**(12): 4150-4156 (1999).

[18] Murillo, E.A. López B.L., Effect of the Maleic Anhydride Content on the Structural, Thermal, Rheological and Film Properties of the n-Butyl Methacrylate–Maleic Anhydride Copolymers, *Prog. Org. Coat.*, **78**: 96-102 (2015).

[19] Nasirtabrizi, M.H., et al., Synthesis and Chemical Modification of Maleic Anhydride Copolymers with Phthalimide Groups, *Hung. J. Ind. Chem.*, **4**(1): 11 (2013).

[20] Becker D ., Hage E., Pessan L., Synthesis and Characterization of Poly (methyl methacrylate-co-maleic anhydride) Copolymers and Its Potential as a Compatibilizer for Amorphous Polyamide Blends, *J. Appl. Polym. Sci.*, **106**: 3248-3252 (2007).

[21] Lee S.-W., Ha C.-S., Cho W.-J., Miscibility of Nylon 6 with Poly (maleic anhydride-co-vinyl acetate) and Hydroxylated Poly (maleic anhydride-co-vinyl acetate) Blends, *Polym. J.*, **37**:3 347-3352 (1996).

[22] Madaeni S.S., Amirinejad S., Amirinejad M., Phosphotungstic Acid Doped Poly (vinyl alcohol)/poly (ether sulfone) Blend Composite Membranes for Direct Methanol Fuel Cells, *J. Membr. Sci.*, **380**: 132-137 (2011).

[23] Lin C., Huang Y., Kannan A., Cross-Linked Poly (vinyl alcohol) and Poly (styrene sulfonic acid-co-maleic anhydride)-Based Semi-Interpenetrating Network as Proton-Conducting Membranes for Direct Methanol Fuel Cells, *J. Power Sources*, **171**: 340-347 (2007).

[24] Pedroza O.J., Dutra Filho J.C., Picciani P.H., Dias M.L., Morphology and Proton Conductivity of Composite Membranes Based on Poly (styrene sulfonic acid–maleic anhydride) Nanofibers Prepared by Electrospinning, *Solid State Ionics*, **21**: 755-764 (2015).

[25] Salarizadeh P., Javanbakht M., Abdollahi M., Naji L., Preparation, Characterization and Properties of Proton Exchange Nanocomposite Membranes Based on Poly (vinyl alcohol) and Poly (sulfonic acid)-Grafted Silica Nanoparticles, *Int. J. Hydrogen Energy*, **38**: 5473-5479 (2013).

[26] Atabaki F., Abdolmaleki A., Barati A., Free Radical Copolymerization of Methyl Methacrylate and N-2-methyl-4-nitro-phenylmaleimide: Improvement in the T g of PMMA, *Colloid. Polym. Sci.*, **294**: 455-462 (2016).

[27] Punuch W., Okhawilai M., Rimdusit S., Property Enhancement of Polybenzoxazine Modified with Maleic Anhydride, *J. Met., Mater. and Miner. (JMMM)*, 24 (2014).

[28] Wang Y., Ma X., Zhang Q., Tian N., Synthesis and Properties of Gel Polymer Electrolyte Membranes Based on Novel Comb-Like Methyl Methacrylate Copolymers, *J. Membr. Sci.*, **349**: 279-286 (2010).

[29] Madaeni S., Rafiee E., Seyedzadeh Z., Barzin J., Effect of Dodeca-Tungstophosphoric Acid on Morphology and Performance of Polyethersulfone Membrane for Gas Separation, *J. Polym. Eng.*, **30**:109-134 (2010).

[30] Li L., Wang Y., Proton Conducting Composite Membranes from Sulfonated Polyethersulfone Cardo and Phosphotungstic Acid for Fuel Cell Application, *J. Power Sources*, **162**(1): 541-546 (2006).

[31] Lafuente E., Piñol M., Martínez M.T., Muñoz E., Oriol L., Serrano J.L., Preparation and Characterization of Nematic Polyazomethine/Single-Walled Carbon Nanotube Composites Prepared by in Situ Polymerization, *J. Polym. Sci., Part A: Polym. Chem.*, **47**: 2361-2372 (2009).

[32] Lishuang X., Hailan H., Meiyu L., Jingmei X., Hongzhe N., Hailong Zh., Da X., Zhe W., Phosphotungstic Acid Embedded Sulfonated Poly (arylene ether ketone sulfone) Copolymers with Amino Groups for Proton Exchange Membranes. *RSC Adv.*, **5**(101): 83320-83330 (2015).

[33] Vijayalekshmi V., Khastgir D., Fabrication and Comprehensive Investigation of Physicochemical and Electrochemical Properties of Chitosan-Silica Supported Silicotungstic Acid Nanocomposite Membranes for Fuel Cell Applications, *Energy*, **142**: 313-330 (2018).

[34] Gang W., Yefeng Y., Guyu X., Deyue Y., Novel Sulfonated Polybenzothiazoles with Outstanding Dimensional Stability for Proton Exchange Membranes, *J. Membr. Sci.*, **425**:200-207 (2013).

[35] Hongtao Li., Gang Z., Chengji Z., Yang Z., Ke S., Miaomiao H., Haidan l., Haidan L., Jing Z., Hui Na., A Novel Sulfonated Poly(ether ether ketone) and Cross-Linked Membranes for Fuel Cells, *J. Power Sources*, **195**(19): 6443-6449 (2010).

[36] Madaeni S.S., Amirinejad S., Amirinejad M., Phosphotungstic Acid Doped Poly (vinyl alcohol)/poly (ether sulfone) Blend Composite Membranes for Direct Methanol Fuel Cells, *J. Member. Sci*, **380**:132-137 (2011).

[37] Peighambardoust S.J., Rowshanzamir S., Amjadi M., Review of the Proton Exchange Membranes for Fuel Cell Applications, *Int. J. Hydrogen Energy*, **35**(17):9349-9384 (2010).

[38] Jiang, J. and O.M. Yaghi, Brønsted Acidity in Metal–Organic Frameworks, *Chem. Rev.*, **115**(14): 6966-6997 (2015).

[39] Yamada M., Honma I., Heteropolyacid-Encapsulated Self-Assembled Materials for Anhydrous proton-Conducting Electrolytes, *J. Phys. Chem. B*, **110**(41): 20486-20490 (2006).

[40] Deuk-Ju K., Hae-Young H., Sam-bong J., Sang-Yong N., Sulfonated Poly (arylene ether sulfone)/Laponite-SO3H Composite Membrane for Direct Methanol Fuel Cell, *J. Ind. Eng. Chem.*, **18**(1): 556-562 (2012).

[41] Lupatini K.N., Schaffer J.V., Machado B., Silva E.S., Ellendersen L.S., Muniz G.I., Ferracin R.J., Alves H.J., Development of Chitosan Membranes as a Potential PEMFC Electrolyte, *Journal of Polymers and the Environment*, 1-9 (2018).